FIELD QUALITY OF THE FERMILAB Nb$_3$Sn HIGH FIELD DIPOLE MODEL*

N. Andreev, D. Chichili, C. Christensen, J. DiMarco, V.V. Kashikhin, P. Schlabach[†], C. Sylvester,
I. Terechkine, J.C. Tompkins, G. Velev, A.V. Zlobin, FNAL, Batavia, IL 60510, USA

Abstract

A short Nb$_3$Sn dipole model based on a single-bore cos-theta coil with a cold iron yoke has been fabricated and tested at Fermilab. Field quality was measured at room temperature during magnet fabrication and at liquid helium temperature. This paper reports the results of magnetic measurements. The geometrical harmonics, coil magnetization effects caused by persistent currents in the superconductor, eddy currents in the cable, and the "snap-back" effect at injection are presented and compared with theoretical predictions.
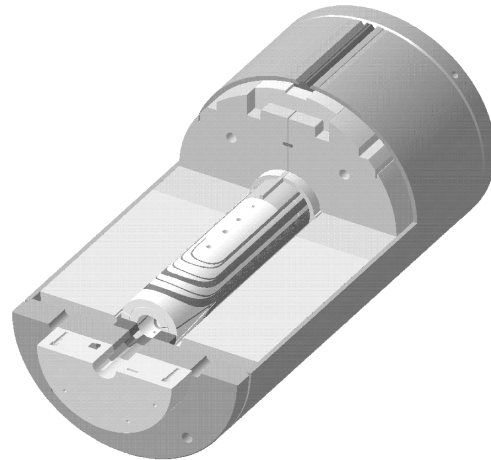
1 INTRODUCTION

High field accelerator magnets are being developed at Fermilab for next generation hadron colliders. These magnets are designed for a nominal field of 10-12 T in the magnet bore of 40-50 mm at the operating temperature of 4.3 K and are based on various design approaches and fabrication techniques [1,2]. To achieve these design parameters, Nb$_3$Sn superconductor is used. One of the design approaches being explored for these magnets is based on a cos-theta coil.

A model magnet program to validate and optimize the magnet design has been undertaken. A 1 m long model magnet (HDFA02) was recently fabricated and is being tested in the Fermilab Vertical Magnet Test Facility. During testing, magnetic measurements were performed both warm and cold. Cold measurements were made at excitation currents up to 7 kA before quench training.

2 MAGNET DESIGN

Magnetic design and parameters of the short model are reported in [3]. The design consists of a two-layer shell-type coil with a 43 mm bore and a cold iron yoke. Fig. 1 is a 3d view of the magnet. The magnet utilizes a keystoned Rutherford-type cable made of 28 Nb$_3$Sn strands, each 1 mm in diameter. The strands were manufactured using the Modified Jelly Roll (MJR) process. Both inner and outer layers of the coil are made from the same cable. The cable has a 25 μm thick stainless steel core to control crossover resistance. A 0.125 mm thick ceramic tape impregnated with liquid ceramic binder is used for cable insulation. The critical current for the virgin strand measured at 12 T and 4.2 K was 726 A, and for extracted strand, 665 A. The critical current degradation in the magnet is 8.5%. Strand and cable RRR was within a range of 7-19.

Figure 1: Two-layer shell-type Nb3Sn dipole model

Each half-coil consists of 24 turns, 11 turns in the inner layer and 13 turns in the outer layer. Two pole posts, one in the inner layer and another one in the outer layer, and four spacers per quadrant, two for each layer, minimize the low order geometrical harmonics in the magnet body. The coil ends also have a blockwise layout of turns with the same number of blocks and turns in the block as in the magnet body. The design goals for the magnet end optimization were stress minimization in the cable blocks and minimization of the end length to increase the magnet straight section for a fixed total coil length.

The iron yoke has an inner diameter of 120 mm and an outer diameter of 400 mm. No special holes for compensation of iron saturation were used in this model. An optimized iron yoke will be used in the next short model. Magnet technology and the details of the short model fabrication are reported elsewhere [4].

3 MEASUREMENT SYSTEM

Magnetic measurements presented in this paper were performed using a vertical drive, rotating coil system with a coil of 2.5 cm nominal diameter and 25 cm length. It has a tangential winding for measurement of field harmonics as well as dedicated dipole windings measuring the lowest order component of the field and allowing for bucking the large dipole component in the tangential winding signal. Coil winding voltages as well as magnet current are read using HP3458 DVMs. DVMs are triggered simultaneously by an angular encoder on the probe shaft, synchronizing measurements of field and current. A centering correction is performed using feed down of

higher order allowed to lower order unallowed harmonics (18, 22 pole to 16, 20 pole).

4 FIELD QUALITY ANALYSIS

In the straight section of the magnet, the field is represented in terms of harmonic coefficients defined by the power series expansion

$$B_y + iB_x = B_1 \times 10^{-4} \sum_{n=1}^{\infty} (b_n + ia_n)\left(\frac{x+iy}{r_0}\right)^{n-1},$$

where B_x and B_y are the transverse field components, B_1 is the dipole field strength, b_n and a_n are the $2n$-pole coefficients ($b_1=10^4$) at a reference radius r_0 of 10 mm. A Cartesian coordinate system is defined with the z axis at the center of the magnet aperture and pointing from return to lead end, the x axis horizontal and pointing to the right of an observer who faces the magnet from the lead end, the y axis pointing upwards.

4.1 Harmonics in the magnet body

Magnet strength measured in the straight section (0.6154 T/kA, warm, 10 A) agrees well with that expected from the design (0.6140 T/kA). The measured magnetic length of 0.803±0.005 m is also in agreement with the calculated value of 0.809 m. A comparison of the geometrical harmonics measured at 3 kA in the magnet body and values calculated for the design geometry is presented in Table 1. Large values of low order harmonics not expected from the design are seen. These are due to asymmetries in the coil assembly introduced during reaction and coil yoking. Harmonics calculated for a plausible as-built model (Fig. 2) are also presented in the table. This geometry shifts the magnet mid-plane by 0.2 mm and introduces a few percent difference in thickness between left and right coil halves.

The residual difference between measured harmonics and those calculated for a plausible as-built geometry are to a large extent consistent with a 50 μm RMS error in block placement (Table 2). Discrepancies in higher order harmonics may be due to the small signal size of this probe, small residual magnetization of the anticryostat or nonlinearity of field harmonics with current.

Table 1: Harmonics in the magnet body. There is no entry for measured b_8 as it was used in the centering correction.

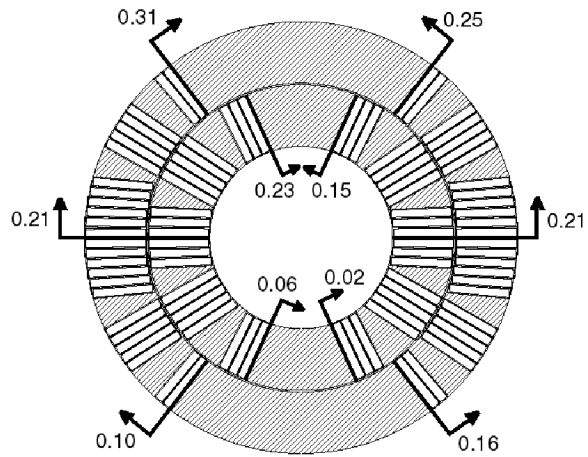|	measured		design values	as built model	
n	a_n	b_n	b_n	a_n	b_n
2	-9.6	4.1	-	-9.5	4.1
3	-0.2	-4.0	0.00	0.0	-4.1
4	-1.1	0.4	-	0.5	0.3
5	0.3	0.0	0.00	0.0	0.0
6	0.3	0.0	-	-0.1	0.0
7	-0.1	0.1	0.00	0.0	0.0
8	-0.2	-	-	0.0	0.0
9	-0.2	-0.2	-0.09	0.0	-0.1

Figure 2: Model of HFDA02 as built which reproduces the measured low order field harmonics. Shifts shown are in units of mm.

Table 2: Comparison of residual field differences to the effects of random block mispositioning

	measured - as built		50μ RMS block error
n	Δa_n	Δb_n	σ_{an}, σ_{bn}
2	-0.1	0.0	1.20
3	-0.2	0.1	0.56
4	-1.7	0.1	0.28
5	0.3	0.0	0.10
6	0.4	0.0	0.05
7	-0.1	0.1	0.02
8	-0.2	-	0.01
9	-0.2	-0.1	0.00

4.2 Coil Magnetization

The effect of coil magnetization on measured harmonics in this magnet is large. For example, the width of the b_3 hysteresis curve is 50 units at 1 kA (Fig. 3). This is due to the high J_c and large effective filament diameter that reaches ~100 microns in Nb_3Sn strands produced using MJR or IT (Internal Tin) processes [5]. Calculations of the magnetization harmonics reproduce measured values over a wide range of currents as shown in Fig. 4 and 5 for the normal sextupole and decapole.
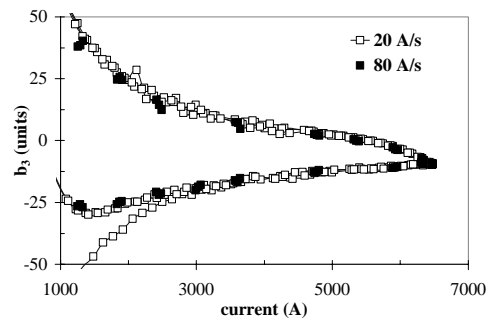

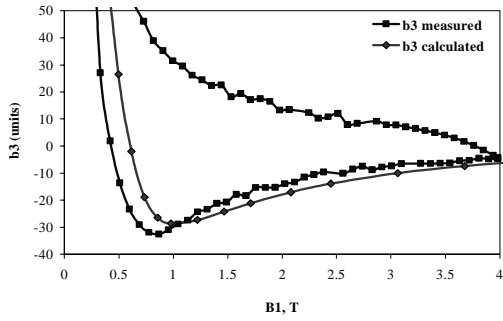Figure 3: Measured b_3 at different ramp rates

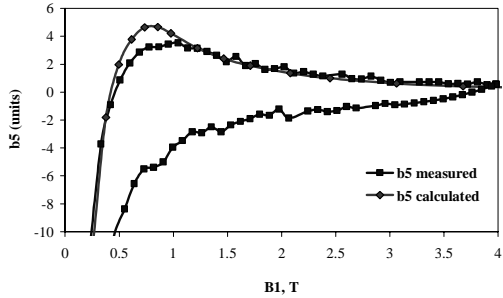Figure 4: Comparison of measured and calculated b_3

Figure 5: Comparison of measured and calculated b_5

To check for dynamic effects during injection, measurements were performed during a 30 min "injection" plateau at 3 kA. The plateau was preceeded by 2 standardization cycles in which the magnet was ramped 0-6500-0 A at a ramp rate of 40 A/s. After a 30 minute plateau at 3 kA, current was increased to 4.5 kA with ramp rate of 5 A/s and then ramped down at 40 A/s. Normal sextupole measurements during this cycle are presented in Fig. 6. Fig. 7 shows the first two allowed harmonics during injection and as the magnet was ramped at the end of the plateau. Changes in the harmonics during injection are very small with respect to those observed in NbTi accelerator magnets [7]. This is not yet understood and will be studied further in this and future models.
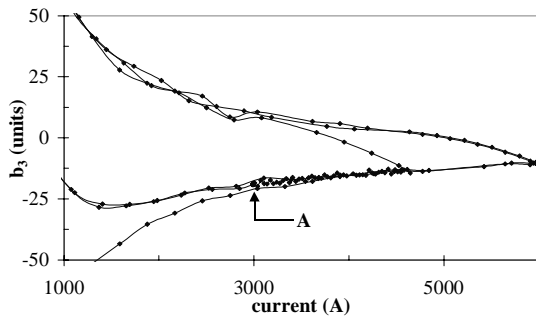
Figure 6: b_3 measured during an accelerator cycle

4.3 Cable eddy currents

Nb$_3$Sn magnets have typically had large eddy current harmonics due to the small crossover resistance created during coil reaction [6]. To control crossover resistance, cable in this magnet has a 25 μm stainless steel core. As can be seen from the agreement between the hysteresis

width of harmonics measurements at 20 and 80 A/s (Fig. 3), eddy currents in this model are resultantly small.
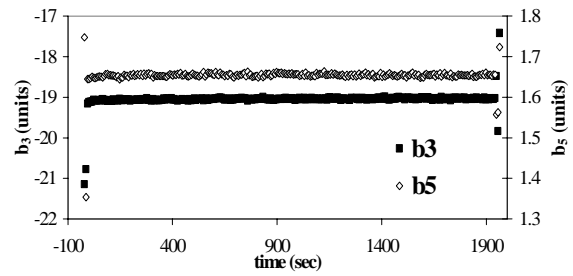
Figure 7: b_3, b_5 near the injection plateau. The current ramp stops at t=0. The first 3 measurements after ramping begins again are also plotted.

5 CONCLUSIONS

Field measurements before quench training of a Nb$_3$Sn model dipole magnet for the Fermilab high field magnet program are consistent with expectations. Body harmonics are consistent with a plausible model of the as-built geometry. The relatively large measured magnetization harmonics are consistent with calculations. A scheme to minimize this with passive correction shims will soon be tested with this model. The pronounced decay and snapback effect seen in NbTi magnets at injection has not been observed. A stainless steel core in the cable has apparently eliminated large eddy current effects seen in other Nb$_3$Sn magnets. Further tests of this model will be performed and additional models in this design series are expected before the end of this year.

6 REFERENCES

[1] A. Zlobin et al., "Development of Cos-theta Nb$_3$Sn Dipole Magnets for VLHC", this conference.

[2] G. Ambrosio et al., "Design and Development of Single-Layer Common Coil Nb$_3$Sn Dipole Magnet for VLHC", this conference.

[3] G. Ambrosio et al., "Magnetic Design of the Fermilab 11 T Nb$_3$Sn Short Dipole Model", IEEE Trans. Appl. Supercond., Vol. 10, No. 1, March 2000, p. 322.

[4] D.R. Chichili et al., "Fabrication of the Shell-Type Nb$_3$Sn Dipole Model at Fermilab", IEEE Trans. Appl. Supercond., Vol. 11, No. 1, March 2001, p. 2160.

[5] E. Barzi et al., "Study of Nb$_3$Sn Strands for Fermilab's High Field Dipole Models", IEEE Trans. Appl. Supercond., Vol. 11, No. 1, March 2001, p. 3595.

[6] A. den Ouden et al., "Application of Nb$_3$Sn Superconductors in High-field Accelerator Magnets", IEEE Trans. Appl. Supercond., Vol. 7, No. 2, June 1997, p. 733.

[7] L. Bottura et al., "Performance of the LHC Final Design Full Scale Superconducting Dipole Prototypes", IEEE Trans. Appl. Supercond., Vol. 11, No. 1, March 2001, p. 1554.